


## RESEARCH ARTICLE

**CASP9 germline mutation in a family with multiple brain tumors**

Michael W. Ronellenfitsch <sup>1,2,3\*</sup>, Ji-Eun Oh<sup>4\*</sup>, Kaishi Satomi<sup>4</sup>, Koichiro Sumi<sup>4</sup>, Patrick N. Harter<sup>2,3,5</sup>, Joachim P. Steinbach<sup>1,2,3</sup>, Jörg Felsberg<sup>6</sup>, David Capper<sup>7,8</sup>, Catherine Voegelé<sup>4</sup>, Geoffroy Durand<sup>4</sup>, James McKay<sup>4</sup>, Florence Le Calvez-Kelm<sup>4</sup>, Jens Schittenhelm<sup>9</sup>, Barbara Klink<sup>10,11,12,13</sup>, Michel Mittelbronn<sup>2,3,5</sup>, Hiroko Ohgaki<sup>4</sup>

<sup>1</sup> Senckenberg Institute of Neurooncology, University Hospital Frankfurt, Frankfurt am Main, Germany.

<sup>2</sup> German Cancer Consortium (DKTK), Heidelberg, Germany.

<sup>3</sup> German Cancer Research Center (DKFZ), Heidelberg, Germany.

<sup>4</sup> International Agency for Research on Cancer (IARC), Lyon, France.

<sup>5</sup> Institute of Neurology (Edinger Institute), Goethe University, Frankfurt am Main, Germany.

<sup>6</sup> Department of Neuropathology, University of Düsseldorf, Düsseldorf, Germany.

<sup>7</sup> Department of Neuropathology, University of Heidelberg, Heidelberg, Germany.

<sup>8</sup> Clinical Cooperation Unit Neuropathology, German Cancer Research Center (DKFZ), Heidelberg, Germany.

<sup>9</sup> Institute of Pathology and Neuropathology, Eberhard-Karls University of Tuebingen, Tuebingen, Germany.

<sup>10</sup> Faculty of Medicine Carl Gustav Carus, TU Dresden, Institute for Clinical Genetics, Dresden, Germany.

<sup>11</sup> German Cancer Consortium (DKTK), Dresden, Germany.

<sup>12</sup> German Cancer Research Center (DKFZ), Heidelberg, Germany.

<sup>13</sup> National Center for Tumor Diseases (NCT), Dresden, Germany.

**Keywords**

astrocytoma, *CASP9*, exome sequencing, Li–Fraumeni-like syndrome.

**Corresponding author:**

Prof. Dr. Michel Mittelbronn, Institute of Neurology (Edinger Institute), Heinrich-Hoffmann-Strasse 7, 60528 Frankfurt am Main, Germany (E-mail: [michel.mittelbronn@kgu.de](mailto:michel.mittelbronn@kgu.de)) and Dr. Hiroko Ohgaki, Head, Section of Molecular Pathology, International Agency for Research on Cancer (IARC), 150 cours Albert Thomas, 69372 Lyon Cedex 08, France (E-mail: [ohgaki@iarc.fr](mailto:ohgaki@iarc.fr))

Received 5 August 2016

Accepted 26 November 2016

Published Online Article Accepted

9 December 2016

\*These authors contributed equally to this work

doi:10.1111/bpa.12471

**Abstract**

We report a novel *CASP9* germline mutation that may increase susceptibility to the development of brain tumors. We identified this mutation in a family in which three brain tumors had developed within three generations, including two anaplastic astrocytomas occurring in cousins. The cousins were diagnosed at similar ages (29 and 31 years), and their tumors showed similar histological features. Genetic analysis revealed somatic *IDH1* and *TP53* mutations in both tumors. However, no germline *TP53* mutations were detected, despite the fact that this family fulfills the criteria of Li–Fraumeni-like syndrome. Whole exome sequencing revealed a germline stop-gain mutation (R65X) in the *CASP9* gene, which encodes caspase-9, a key molecule for the p53-dependent mitochondrial death pathway. This mutation was also detected in DNA extracted from blood samples from the two siblings who were each a parent of one of the affected cousins. Caspase-9 immunohistochemistry showed the absence of caspase-9 immunoreactivity in the anaplastic astrocytomas and normal brain tissues of the cousins. These observations suggest that *CASP9* germline mutations may have played a role at least in part to the susceptibility of development of gliomas in this Li–Fraumeni-like family lacking a *TP53* germline mutation.

**INTRODUCTION**

The etiology of astrocytic glioma is poorly understood. The few known risk factors include exposure to therapeutic ionizing radiation and several rare hereditary tumor syndromes, such as Li–Fraumeni syndrome and Li–Fraumeni-like syndrome, caused by *TP53* germline mutations; tuberous sclerosis complex, caused by *TSC1/2* germline mutations; and neurofibromatosis type I, associated with *NFI* germline mutations (23, 24, 26).

Li–Fraumeni syndrome is an autosomal dominant disorder characterized by multiple primary neoplasms (predominantly soft tissue sarcomas, osteosarcomas, and breast cancer) in children and young adults, with an increased incidence of brain tumors, leukemia, and adrenocortical carcinomas (17). The clinical criteria of Li–Fraumeni syndrome are (i) occurrence of sarcoma before the age of 45 years, (ii) at least one first-degree relative with any tumor before the age of 45 years, and (iii) a first- or second-degree relative with

cancer before the age of 45 years or sarcoma at any age (17). Several less stringent sets of criteria, for example the Birch criteria, the second definition by Eeles, and the Chompret criteria, have been proposed to identify more families with *TP53* germline mutations (17). Individuals who fulfill these criteria are considered to have Li–Fraumeni-like syndrome.

Brain tumors are the fourth most frequent neoplasms in families with Li–Fraumeni syndrome, and account for approximately 13% of all tumors with *TP53* germline mutations (16). Several families with *TP53* germline mutations have shown remarkable clustering of brain tumors (13, 34, 37). We recently reported that germline mutations of *TP53*, *MSH4*, and *LATS1* were co-present in a family with Li–Fraumeni syndrome with multiple central nervous system tumors. All three of the family members with glioma carried *MSH4* and *TP53* germline mutations, whereas two family members with schwannoma had *MSH4* and *LATS1* germline mutations (13).

We here report a family with Li–Fraumeni-like syndrome lacking *TP53* germline mutation in which three brain tumors and a case of leukemia have been diagnosed. Two young adult female cousins in the family developed anaplastic astrocytoma (WHO grade III) in the right brain hemisphere at the ages of 29 and 31 years. This is a remarkable observation because anaplastic astrocytoma is a rare tumor, with an annual incidence per 100 000 population of 0.56 cases in the USA (27) and 0.25 cases in Europe (25). In this study, we performed exome sequencing using blood samples from the cousins and several other family members to identify novel germline mutations that increase susceptibility to the development of brain tumors.

## MATERIALS AND METHODS

### Immunohistochemical characterization of anaplastic astrocytomas

Immunohistochemistry was performed using antibodies against GFAP, MAP2, Ki67, pHH3, p53, ATRX, and IDH1 (R132H), using the Discovery XT system (Ventana/Roche, Strasbourg, France) according to standard diagnostic protocols. The following antibodies were used: polyclonal rabbit anti-human GFAP (astrocytic glial fiber acid protein; dilution 1:20 000; clone Z0334; Dako, Glostrup, Denmark), monoclonal mouse anti-human MAP2 (dilution 1:3000; clone AP-20; Sigma-Aldrich, Munich, Germany), monoclonal mouse anti-human Ki67 (dilution 1:200; clone MIB-1; Dako, Glostrup, Denmark), polyclonal rabbit anti-human pHH3 (dilution 1:100; 06-570; EMD Millipore, Billerica, MA, USA), monoclonal mouse anti-human p53 (dilution 1:500; clone DO7, BP53-12; NeoMarkers, Fremont, CA, USA), polyclonal rabbit anti-ATRX (dilution 1:200; HPA001906; Sigma-Aldrich, St. Louis, MO, USA), and monoclonal mouse anti-human mIDH1 R132H (dilution 1:50; clone H09; Dianova GmbH, Hamburg, Germany).

### Genetic characterization of anaplastic astrocytomas

#### *TP53* mutation, *IDH1* mutation, *CDKN2A* (*p16<sup>INK4a</sup>*) homozygous deletion

Screening for *TP53* mutations (exons 4–10) in the anaplastic astrocytomas from patients P and Q was carried out using Sanger

sequencing, as previously described (12, 35). Screening for *IDH1* mutations was carried out using Sanger sequencing as previously described (36). Screening for *CDKN2A* (*p16<sup>INK4a</sup>*) homozygous deletion was performed using differential PCR ( $\beta$ -actin sequence as a reference), as previously described (21, 38).

#### 450k methylome analysis and copy number profiling

The Infinium HumanMethylation450 (450k) array (Illumina, San Diego, CA, USA) was used, according to the manufacturer's instructions, to determine the DNA methylation status of 482 421 CpG sites, at the Core Facility of the German Cancer Research Center (DKFZ) in Heidelberg, Germany. The methylation level of each CpG site was represented by  $\beta$ -values, which ranged from 0 (unmethylated) to 1 (fully methylated). CpG sites with  $\beta$ -values of 0.4 or more were considered to be methylated. Genome-wide copy-number profiles were determined using the intensity measures of the aforementioned methylation probe loci throughout the genome. Chromosomal copy-number alterations were visualized using the IdeogramBrowser tool (20).

#### Exome sequencing to detect novel germline mutations

Genomic DNA was extracted from blood samples from the patients with anaplastic astrocytoma (P and Q) and their family members (E and M) and 1.5  $\mu$ g was used for whole exome sequencing library preparation according to the Life Technologies SOLiD Fragment Library Preparation protocol (PN 4460960 Rev. A), with some modifications. The protocol was adapted such that all reagent volumes were halved. Briefly, 1.5  $\mu$ g of each DNA sample was sonicated into small fragments (with a mean length of 160 bp) in 60  $\mu$ L using the Covaris S220 System. The 60  $\mu$ L of the sheared products was then end-polished by addition of 40  $\mu$ L of the master mix, and then size-selected using Agencourt AMPure XP magnetic beads to specifically retain DNA fragments measuring 100–250 bp. A dA tail was added to the size-selected DNA fragments, and barcoded adaptors were then ligated before purification using the Agencourt AMPure XP magnetic beads. The purified ligated products were then amplified with six cycles of polymerase chain reaction and subsequently purified using the Agencourt AMPure XP magnetic beads. Quality controls included (i) quantitation of DNA after size selection, ligation of adaptors, and amplification of DNA fragments, using the Qubit dsDNA HS Assay Kit and the Qubit 2.0 Fluorometer, and (ii) DNA profiling of the DNA fragments at the same steps using the Agilent High Sensitivity DNA Kit and the Agilent Technologies 2100 Bioanalyzer. The purified barcoded ligated products (62.5 ng) were pooled. Exome capture was performed following the Life Technologies Ion TargetSeq Exome Enrichment System protocol (MAN0006730) using the Ion TargetSeq Exome Enrichment Kit. The pooled barcoded library (125 ng) was hybridized to 2.5  $\mu$ L of Ion TargetSeq Exome probe pool in buffers for 72 h at 47°C, and the probe-hybridized DNA was then washed and recovered using Dynabeads M-270 Streptavidin beads in 15  $\mu$ L of nuclease-free water. This pool was then nick-translated and amplified with eight cycles of polymerase chain reaction using WildFire primers (Life Technologies, Foster City, CA, USA) and was purified using Agencourt AMPure XP magnetic beads in Low TE buffer (15  $\mu$ L). The pooled library (4 nM) was then hybridized

to two lanes of a SOLiD 5500WF FlowChip, and the template amplification was performed semi-automatically, according to the manufacturer's instructions (PN 4477195 Rev. B). Paired-end sequencing runs of 50 bp × 50 bp were conducted on a SOLiD 5500WF Genetic Analysis System (Life Technologies by Thermo Fisher Scientific, Waltham, MA, USA). The exome sequencing analyses were performed at the IARC Genetic Platform.

### Bioinformatic analyses

Exome data analyses (mapping and variant calling) were performed using a combination of LifeScope targeted resequencing and low frequency variant detection workflows, with the default parameters: (i) the color space reads generated by the SOLiD 5500WF system were mapped against the human genome reference version hg19, generating BAM files, which were then enriched for targets and good-quality reads, and (ii) single-nucleotide variants (SNVs) were called on enriched BAM files in both targeted resequencing and low frequency variant detection, and small insertions and deletions (indels) were called on enriched BAM files in the targeted resequencing workflow. Using the Annovar software, the Variant Call Format (VCF) output files were then annotated with functional annotations as well as frequencies in known databases and in our custom "SOLID WildFire" catalog of variants. To remove recurrent false-positive calls and common variants, we excluded from these annotated lists of variants any variant found in >10% of the 36 different samples that were previously sequenced at the International Agency for Research on Cancer (IARC) on the SOLiD 5500WF platform, and from which we generated a catalog of mutations. Additional quality filtering excluded variants with (i) read depth less than 5, (ii) fewer than three different sequence read starting points, and (iii) genomic super dups (reflecting repetitive genomic regions) over 0.9 (this filter was applied to SNVs only). Variants with unknown frequencies or reported frequencies of <1% in the 1000 Genomes database (<http://www.1000genomes.org/>) were retained and then filtered further based on the following refGene annotation criteria: (i) inclusion of SNVs that generate or abrogate exonic nonsense mutations, (ii) inclusion of small indels that generate exonic frameshift and non-frameshift mutations, (iii) inclusion of non-synonymous SNVs with a deleterious score predicted by SIFT (<http://sift.jcvi.org/>) (15, 22) or PolyPhen-2 (<http://genetics.bwh.harvard.edu/pph2/index.shtml>) (1), and (iv) inclusion of SNVs that disrupt the splicing process. Selected candidate genetic alterations were also evaluated with the PMut software (<http://mmb.pcb.ub.es/PMut/>) (4).

### Validation of exome sequencing data by Sanger sequencing

To validate the genetic alterations detected by exome sequencing, we performed Sanger sequencing using blood DNA samples from individuals E, M, P, and Q (used for exome sequencing), blood DNA samples from additional family members (K, L, and N), blood DNA samples from 10 healthy individuals unrelated to the family, and tumor DNA samples from anaplastic astrocytomas of patients P and Q. Sanger sequencing was performed on an ABI PRISM 3100 Genetic Analyzer (Applied Biosystems, Foster City, CA, USA) with the BigDye Terminator Cycle Sequencing Kit

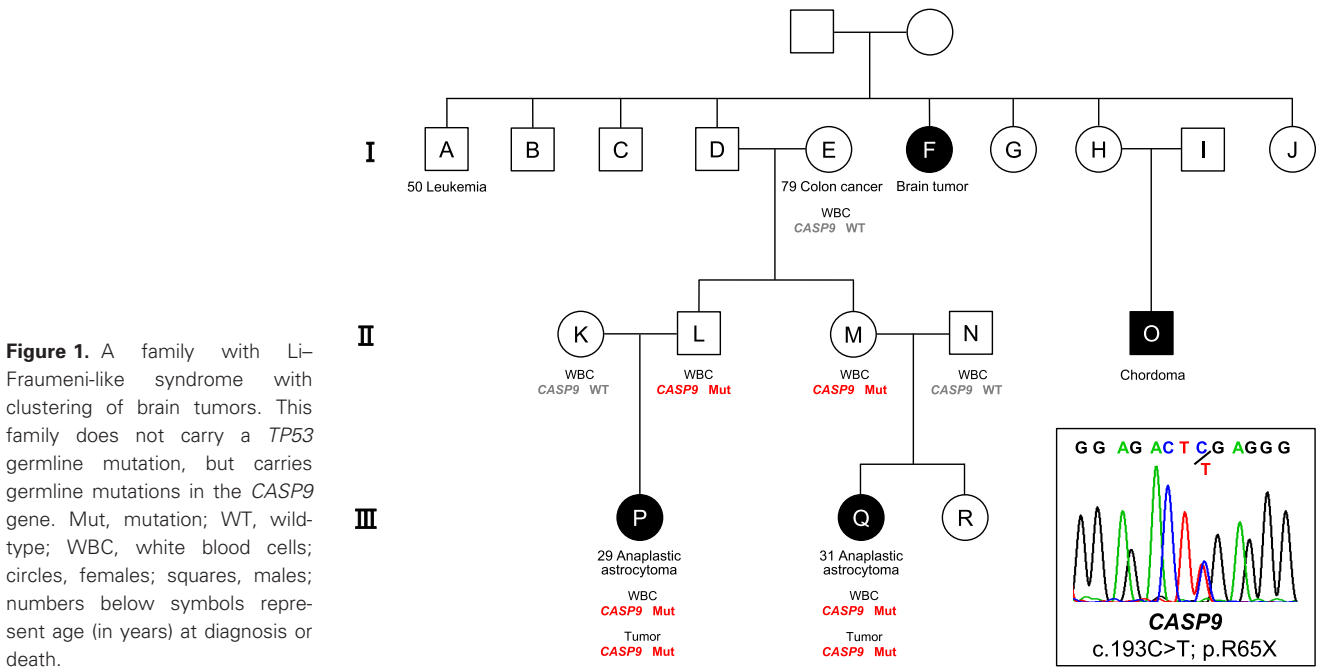
(ABI PRISM, Applied Biosystems), as previously reported (2). The primer sequences are listed in Supporting Information Table S1.

### *CASP9* promoter methylation

Promoter methylation of the *CASP9* gene was determined by methylation-specific PCR (8). Based on information of the *CASP9* promoter region provided by Ensembl genome browser (ENSR00001742967, <http://www.ensembl.org/>) (39), sequences of promoter region and CpG islands of the *CASP9* gene were identified using UCSC Genome Browser (GRCh37/hg19, <http://genome.ucsc.edu/>) (11). Primers for the methylation-specific PCR were designed in chr1:15851107-15851581. Blood DNA and tumor DNA samples from the patients with anaplastic astrocytoma (P and Q), positive controls (CpGenome™ Universal Methylated DNA, Millipore, Temecula, CA, USA), and negative controls (DNA extracted from normal blood samples from unrelated healthy individuals) were treated with bisulfite using the EZ DNA Methylation™ Kit (ZYMO RESEARCH, Irvine, CA), as described previously (40). PCR was carried out in a total volume of 10 µl, with initial denaturation at 94°C for 1 minute, which was followed by 40 cycles consisting of denaturing at 94°C for 15 s, annealing at 60°C for 15 s, and extension at 68°C for 30 s. A final extension was added at 72°C for 5 minutes. Primer sequences were 5'-TTT CGG GAC GTA TTT AGA AGG TTT C-3' (forward) and 5'-TAA ATC CTA AAA ACG AAA CGA TAA CG-3' (reverse) for methylated reaction (PCR product, 137 bp), and 5'-TTT GGG ATG TAT TTA GAA GGT TTT G-3' (forward) and 5'-AAA TTA AAT CCT AAA AAC AAA ACA ATA ACA-3' (reverse) for unmethylated reaction (140 bp). The amplified products were electrophoresed on 2% agarose gels, and were visualized with Gel-Red™ Nucleic Acid Gel Stain. Positive and negative controls were included for each reaction.

### Caspase-9 immunohistochemistry

Paraffin sections were deparaffinized in xylene and 95% ethanol for 5 minutes. After inactivation of endogenous peroxidases with 3% H<sub>2</sub>O<sub>2</sub> in methanol for 30 minutes, the sections were incubated in epitope retrieval solution (diluted 1:10; H-3300; low pH 6.0; Vector Laboratories, Burlingame, CA, USA) for 20 minutes at 95–99°C. The sections were cooled for 40 minutes at room temperature, then incubated overnight at 4°C with anti-caspase-9 antibody (diluted 1:25; HPA001473; rabbit polyclonal; Sigma-Aldrich, St. Louis, MO, USA) diluted in antibody diluent (S3022; Dako, Les Ulis, France). This antibody is targeted against a protein sequence corresponding to amino acids 141–272 of caspase-9. The sections were then washed in phosphate-buffered saline and incubated with the secondary antibody (EnVision+ Single Reagents HRP rabbit; K4002; Dako, Les Ulis, France) for 30 minutes. Visualization was performed over the course of 4 minutes, using the Vector DAB Substrate Kit (SK-4100; Vector Laboratories). After being washed in phosphate-buffered saline, the sections were counterstained with hematoxylin. Several positive controls were used to optimize the immunohistochemistry protocols and the interpretation of the absence of immunoreactivity for caspase-9: normal human colon, glioblastoma, and normal human brain from unrelated individuals with wildtype *CASP9*. Human liver tissue was used as a negative control.



**CASE AND FAMILY HISTORIES**

The female patients, P and Q, are cousins (Figure 1) who grew up in different parts of Germany. Patient P had a history of migraine for many years. Her initial symptom, aura without headache, presented at the age of 29 years; 4 months later, the patient developed numbness of the left leg and an increased frequency of migraine episodes. Magnetic resonance imaging showed a right frontal mass lesion. The patient underwent gross total tumor resection, and the tumor was diagnosed as anaplastic astrocytoma (WHO grade III). The patient received adjuvant treatment consisting of radiotherapy (a total dose of 59.4 Gy) and concomitant temozolomide, as a participant in the CATNON trial (EORTC 26053-22054). The patient was recurrence free as of March 2016.

Patient Q had no relevant pre-existing illness. Her initial symptoms were numbness of the left leg and decline of psychophysical capacity, at the age of 31 years. Magnetic resonance imaging showed a right postcentral mass lesion, and the patient underwent subtotal tumor resection. The tumor was diagnosed as diffuse astrocytoma (WHO grade II). No adjuvant therapy was administered. Four months later, radiological imaging revealed signs of tumor regrowth with malignant progression. Gross total tumor resection was achieved, and the recurrent tumor was diagnosed as anaplastic astrocytoma (WHO grade III). The patient received adjuvant therapy consisting of nine cycles of temozolomide on a 150–200 mg/m<sup>2</sup> 5/28 day dosing schedule, consistent with the adjuvant temozolomide dosing schedule used in the EORTC 22981-26981 trial (32). The tumor recurred after 39 months. Another resection was performed and histology again showed an anaplastic astrocytoma, with similar morphological features but slightly higher mitotic and proliferation indexes.

The parents of patient P (K and L) and patient Q (M and N) are healthy (Figure 1). The grandfather (D) of both P and Q died with no evidence of tumor, at 92 years of age. Their grandmother (E) was diagnosed with colon cancer at 79 years. The grandfather had a brother (A) who died of leukemia at 50 years of age and a sister

(F) who had had a brain tumor (age and histological type unknown). Another sister (H) of the grandfather had a son (O) who had a chordoma.

**RESULTS**

**Histological features and immunophenotype of anaplastic astrocytomas**

The histological features and immunophenotype of the anaplastic astrocytomas in patient P (Figure 2A–H) and patient Q (Figure 2I–P) were highly similar. Both tumors were diffusely infiltrating glial tumors with moderately to highly elevated cell density and moderate nuclear pleomorphism, with a matrix showing a partly microcystic, loosened texture (Figure 2A,I). The astrocytic origin of the tumors was confirmed by strong GFAP expression (Figure 2B,J) and slightly weaker MAP2 positivity in tumor cell processes (Figure 2C,K). Both astrocytomas displayed only infrequent mitotic figures (Figure 2D,L) and had a Ki67 proliferation index focally reaching 5% (Figure 2E,M). Most tumor cells presented with strong expression of p53 (Figure 2F,N) and IDH1 R132H (Figure 2G,O), but lacked nuclear ATRX (Figure 2H,P).

**Genetic profile of anaplastic astrocytomas**

*TP53* mutations were detected by Sanger sequencing at codon 127 (c.379T > C; p.S127P; homozygous) in the anaplastic astrocytoma from patient P, and at codon 273 (c.817\_818CG > TA; p.R273Y; heterozygous) in the anaplastic astrocytoma from patient Q (Table 1). *IDH1* mutation at codon 132 (c.395G > A; p.R132H) was detected in the anaplastic astrocytomas of both patients (Table 1). Mutations in the *TP53* and *IDH1* genes were absent in blood samples from both patients, indicating that the mutations were somatic.

450k analysis revealed the typical methylation profile of astrocytoma with *IDH* mutations in the tumors from both patients. In the

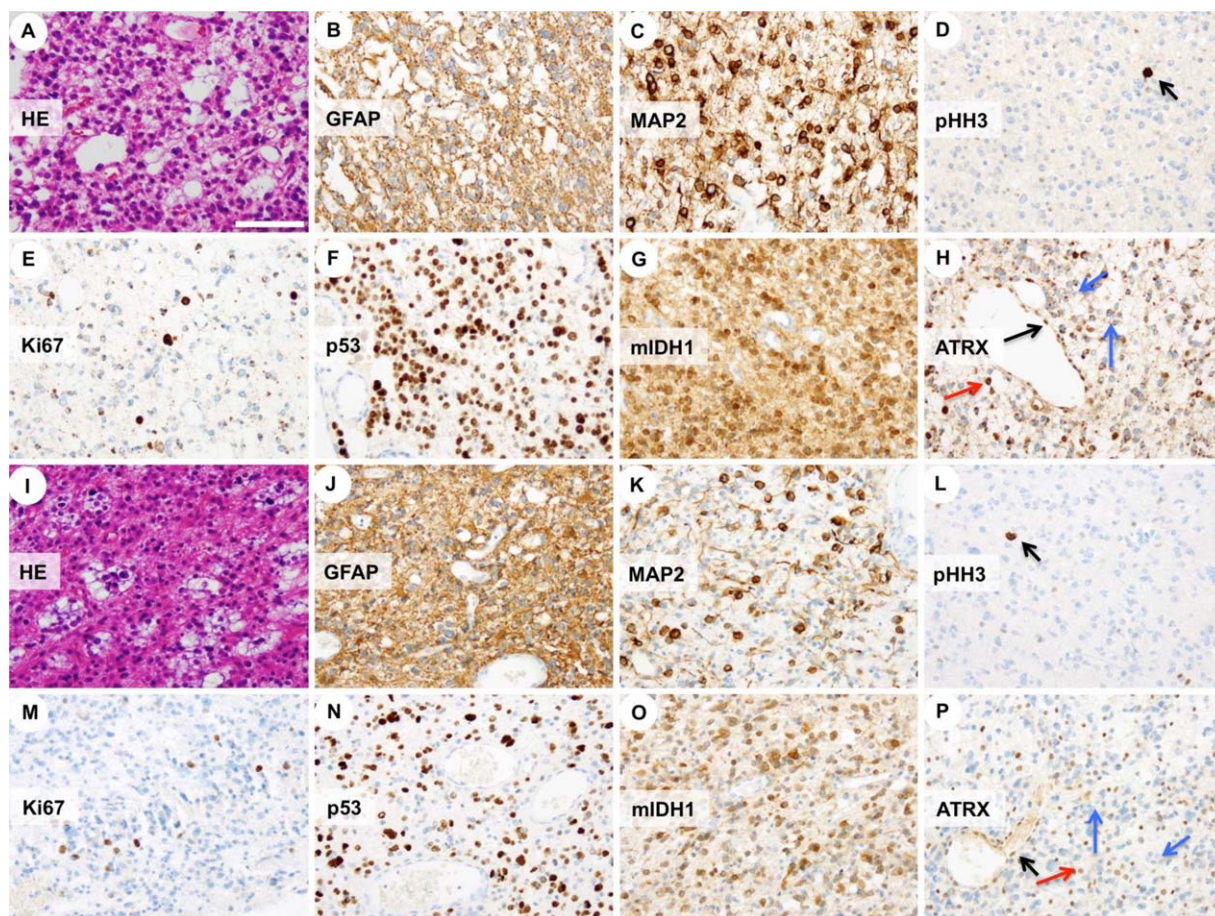


**Figure 2.** Neuropathological features of anaplastic astrocytomas in cousins. Histology and immunohistochemistry of the anaplastic astrocytomas in patient P (**A–H**) and Q (**I–P**). Hematoxylin and eosin (HE) staining shows neuroepithelial tumors with moderate to focally higher cell density and microcystic alterations (**A, I**). The glial origin of the tumor was confirmed by the immunopositivity for GFAP (**B, J**) and MAP2 (**C, K**) in cellular processes. Both tumors displayed infrequent pHH3-positive mitotic figures (**D, L**; black arrows). The Ki67

proliferation index focally reached 5% (**E, M**). Most tumor cell nuclei were strongly p53-positive (**F, N**), consistent with the presence of *TP53* somatic mutations (Ser127Pro in patient P and Arg273Tyr in patient Q). The tumor cells expressed IDH1 R132H (**G, O**) and displayed nuclear loss of ATRX (**H, P**; blue arrows), whereas endothelial cells (**H, P**; black arrows) and residual glial cells (**H, P**; red arrows) presented with ATRX-positive nuclei.

anaplastic astrocytoma from patient P, gains were observed at chromosomes 7q, 16q, and 20q, and losses were detected at 7q, 9p, 13q, 18p, 19q, and 22q (Figure 3A; Table 1). The anaplastic astrocytoma from patient Q displayed gains at chromosomes 8p, 15q, and 19q and losses at 6q, 8p, 9p, and 19q (Figure 3B; Table 1).

Differential PCR also showed the loss at the *CDKN2A* locus at 9p in both anaplastic astrocytomas, but not in blood samples from both patients, indicating that *CDKN2A* loss is somatic.

### Exome sequencing to detect novel germline mutations

We hypothesized that the two cousins with anaplastic astrocytoma (P and Q), as well as patient Q’s mother (M) and patient P’s father (L) were likely carriers of genetic alterations that confer increased susceptibility to brain tumor development, whereas the cousins’ grandmother (E) was considered a non-carrier. We identified rare

**Table 1.** Somatic genetic alterations in anaplastic astrocytomas in cousins.

	Patient P	Patient Q
<i>TP53</i> mutation	Codon 127 (TCC→CCC, Ser→Pro)	Codon 273 (CGT→TAT, Arg→Tyr)
<i>IDH1</i> mutation	Codon 132 (CGT→CAT, Arg→His)	Codon 132 (CGT→CAT, Arg→His)
450k profile	Astrocytic tumor	Astrocytic tumor
Chromosomal gain	7q, 16q, 20q	8p, 15q, 19q
Chromosomal loss	7q, 9p, 13q, 18p, 19q, 22q	6q, 8p, 9p, 19q

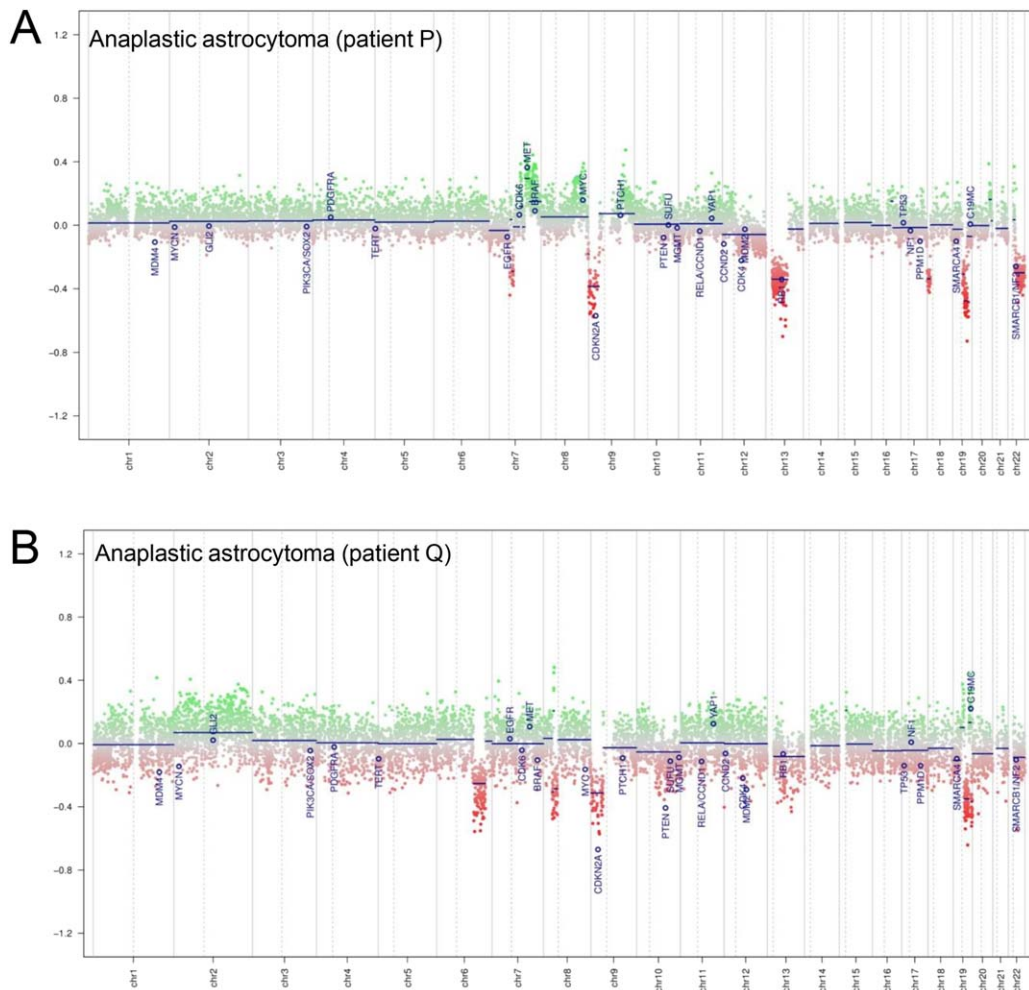


**Figure 3.** Copy number profile generated by 450k methylome analysis of anaplastic astrocytomas from patient P (A) and patient Q (B). Loss of chromosomes 9 and 19 are apparent in the tumors from both patients.

germline variants common to P, Q, and M in 20 genes: *ALMS1*, *C19orf57*, *CASP9*, *CYSLTR1*, *DMTF1*, *FGF11*, *MRPS17*, *NOP16*, *OR11H6*, *PDHB*, *PITPNM3*, *POR*, *PPIL1*, *RNF39*, *RSPO2*, *SLC44A2*, *STK31*, *TP53BP2*, *TYK2*, and *ZZEF1*. Characterization of the deleterious nature of all these variants was scored using Combined Annotation Dependent Depletion (CADD) score (14). The variants in 17 genes with CADD score  $\geq 20$  which indicates the 1% most deleterious were selected, while variants in the *OR11H6*, *ALMS1* and *CYSLTR1* genes were excluded because of their low CADD score. Then we prioritized candidate genes according to their functions, using information in the GeneCards (<http://www.genecards.org/>) and UniProt (<http://www.uniprot.org/>) databases. As a result, 12 genes (*CASP9*, *DMTF1*, *FGF11*, *NOP16*, *PDHB*, *PITPNM3*, *PPIL1*, *RSPO2*, *STK31*, *TP53BP2*, *TYK2*, and *ZZEF1*) were chosen. Of these, *FGF11*, *NOP16*, *PPIL1*, *RSPO2*, *STK31*, and *ZZEF1* were subsequently excluded because their allelic frequency was less than 25% in blood samples from individuals P, Q, and M, suggesting false-positive results. The remaining six genes (*CASP9*, *DMTF1*, *PDHB*, *PITPNM3*, *TP53BP2*, and *TYK2*) were selected for validation by Sanger sequencing.

Germline mutations in *CASP9* (1p36.21), *TP53BP2* (1q41), *DMTF1* (7q21), and *PITPNM3* (17p13) were confirmed by Sanger sequencing to be present in family members M, P, and Q, but were absent in family member E and in the blood DNA samples from 10 healthy unrelated individuals.

A *CASP9* germline stop-gain mutation (NM\_001229.4; c.193C > T; p.R65X), leading to protein truncation, was identified in the caspase recruitment domain, which is essential for binding with APAF1 (30). *CASP9* encodes caspase-9, which is a key molecule for the p53-dependent mitochondrial death pathway (19). Notably, this p.R65X mutation results in loss of the catalytic domain of caspase-9 (<http://www.uniprot.org/uniprot/P55211>). All mutations were heterozygous. This mutation was not reported in the 1000 Genomes database or in the Exon Variant Server (<http://evs.gs.washington.edu/EVS/>), and was found in only 1 of 121 212 studied alleles (allele frequency:  $8.25 \times 10^{-4}\%$ ) in the Exome Aggregation Consortium (ExAC) browser (<http://exac.broadinstitute.org/>). Immunohistochemistry showed the absence of caspase-9 immunoreactivity in the anaplastic astrocytomas and normal brain tissues of patients P and Q, whereas gliomas (one IDH-wildtype glioblastoma, one IDH-mutant glioblastoma, two IDH-mutant

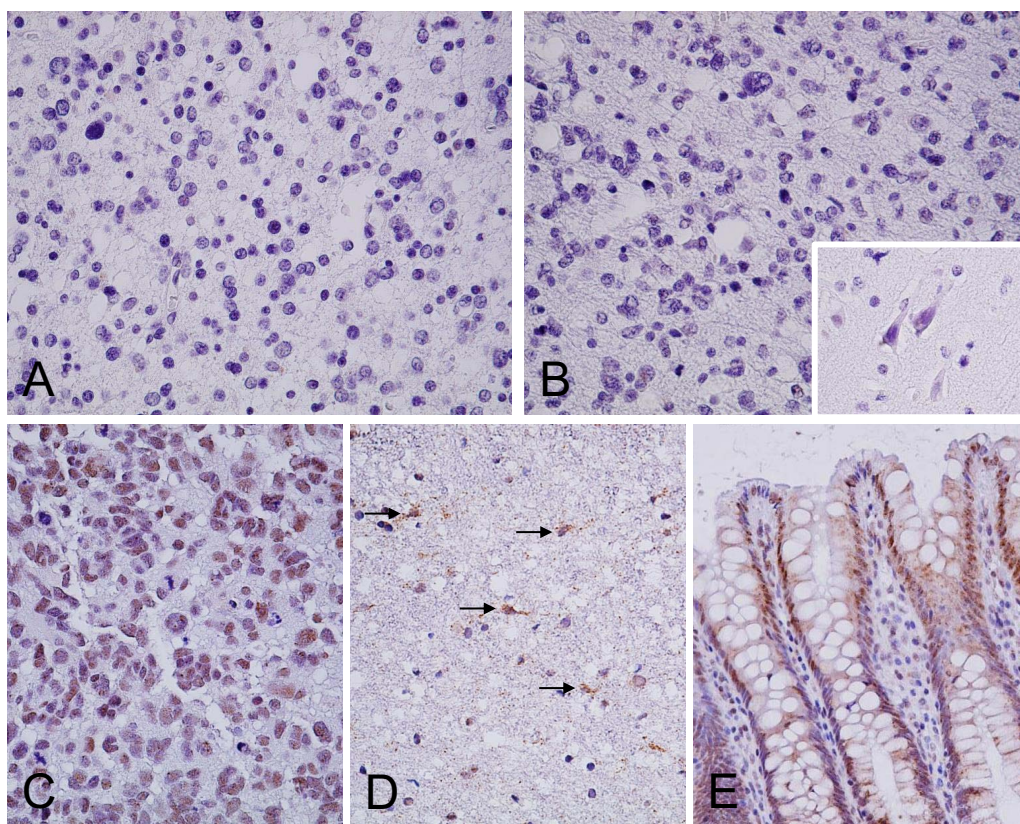


**Figure 4.** Immunohistochemistry showing the absence of immunoreactivity for caspase-9 in the anaplastic astrocytoma of patient P (A) and in the anaplastic astrocytoma (B) and peritumoral normal brain tissue (B, inset) of patient Q. Both P and Q are carriers

of a *CASP9* germline stop codon mutation. Caspase-9 is expressed in the positive controls: glioblastoma (C), astrocytes (arrows) in normal brain (D), and columnar epithelial cells in normal colon (E) from unrelated individuals with wildtype *CASP9*.

anaplastic astrocytomas, and one IDH-mutant low-grade astrocytoma) and normal brain tissues from unrelated individuals with wild-type *CASP9* were immunoreactive for caspase-9 (Figure 4). Methylation-specific PCR revealed that the *CASP9* promoter was unmethylated in both blood and anaplastic astrocytoma DNA samples from patients P and Q.

A *PITPNM3* (encoding a phosphatidylinositol transfer membrane-associated protein) germline missense mutation (NM\_031220.3; c.1688C > T; p.T563M; rs139119218 in the dbSNP database) was in the DDHD domain. This domain is located within a longer C-terminal region that binds to PYK2 tyrosine kinase. All the mutations were heterozygous except for that in the anaplastic astrocytoma from patient P, which showed the absence of the wildtype base, suggesting loss of the wildtype allele. The frequency of this mutation in the normal population is 0.1% in the 1000 Genomes database, and the allele frequency is 0.04% (53/118 276 studied alleles) in the ExAC browser. PolyPhen-2 and SIFT predicted that this mutation is damaging, and PMut predicted it is pathological.

A *TP53BP2* (encoding ASPP2) germline missense mutation (NM\_001031685.2; c.1902G > C; p.Q634H; rs61824007; dbSNP database <http://www.ncbi.nlm.nih.gov/snp/>) was identified near the proline-rich region, which is important for regulating the interaction of ASPP2 with p53 (29). Except for a homozygous mutation in patient P, the mutations were heterozygous. The frequency of this

mutation in the normal population is 1% in the 1000 Genomes database, and the allele frequency is 0.8% (1001/121 364 studied alleles) in the ExAC browser. PolyPhen-2 predicted that this mutation is damaging, whereas SIFT predicted it is tolerated and PMut predicted it is neutral.

A *DMTF1* germline missense mutation (NM\_001142327.1; c.286G > C; p.A96P; rs117360089 in the dbSNP database) was identified in the DNA-binding domain, which is essential for the encoded protein's interaction with p53 (5). All mutations were heterozygous. The frequency of this mutation in the normal population is 1% in the 1000 Genomes database, and the allele frequency is 1.6% (1974/121 216 studied alleles) in the ExAC browser. SIFT predicted that this mutation is damaging, whereas PolyPhen-2 predicted it is benign and PMut predicted it is neutral.

## DISCUSSION

We present a remarkable family in which three brain tumors had developed within three generations, including two anaplastic astrocytomas occurring in cousins. These anaplastic astrocytomas were diagnosed at similar patient ages and showed similar histological features. Genetic analysis showed somatic *IDH1* and *TP53* mutations in both tumors. However, no germline *TP53* mutations were detected, despite the fact that this family meets the criteria for

Li–Fraumeni-like syndrome according to both the second definition by Eeles and the Chompret criteria (7).

To identify novel germline mutations associated with susceptibility to brain tumor development, we carried out exome sequencing using blood samples from family members, including the cousins with anaplastic astrocytoma, and detected several candidate germline mutations. Of these, a *CASP9* stop-gain (p.R65X) was the only mutation predicted to have functional consequences by all three prediction tools used, and appears to damage the p53 signaling pathway. *CASP9* germline stop-gain mutation results in a truncated caspase recruitment domain for binding with APAF1 and absence of the catalytic domain (19). Furthermore, caspase-9 expression was not detectable by immunohistochemistry in anaplastic astrocytomas and normal brain tissue of the cousins, despite the presence of one wild-type allele and absence of *CASP9* promoter methylation. This may be explained by haploinsufficiency and very low expression, i.e. lower than detectable level by immunohistochemistry.

*CASP9* encodes caspase-9, which is a key molecule for the p53-dependent mitochondrial death pathway (19). In response to DNA damage, p53 transcriptionally promotes pro-apoptotic molecules (e.g., Bax, PUMA, and Bak) and inhibits anti-apoptotic proteins (Bcl-2 and Bcl-XL) (33). This leads to the mitochondrial release of cytochrome c, which interacts with APAF1 and caspase-9 to form a complex called the apoptosome, which activates caspase-9. Activated caspase-9 subsequently triggers a cascade of effector caspases (i.e., caspase-3, -6, and -7), resulting in cell death (28). Furthermore, caspase-9 is also known as a key downstream molecule of other signaling pathways, such as PI3K/AKT (9, 18) and endoplasmic reticulum (ER) stress pathways (10).

It has been reported that *CASP9* deletion results in perinatal lethality in mice, with increased brain size due to neuronal hyperplasia, grossly abnormal brain development, and defective mitochondria-mediated apoptosis of the proliferative neuroepithelium (19). Mouse embryo fibroblasts deficient in caspase-9 have been shown to be resistant to apoptotic stimuli, and the inactivation of caspase-9 has been shown to transform mouse embryo fibroblasts (31).

This study suggests that *CASP9* germline mutations may link to susceptibility to development of brain tumors in a Li–Fraumeni-like family lacking a *TP53* germline mutation. However, loss of caspase 9 alone may not be sufficient for development of brain tumors, since there are family members carrying a *CASP9* mutation without disease. This view is supported by The Cancer Genome Atlas (TCGA) data, showing that *CASP9* mutations are absent or infrequent in human neoplasms (occurring in <5% of cases). A *CASP9* missense mutation was found in only 1 of 267 IDH-wildtype glioblastomas (3, 6). It remains to be shown whether co-presence of other germline mutations detected in this study contributed to susceptibility of development of multiple brain tumors in this family.

In summary, this study provides novel evidence that germline *CASP9* mutation is present in a family with Li–Fraumeni-like syndrome with multiple brain tumors. Genome-wide sequencing of blood samples from families with Li–Fraumeni or Li–Fraumeni-like syndrome lacking *TP53* germline mutations or those with remarkable clustering of certain cancer types may identify additional novel cancer susceptibility genes.

## REFERENCES

- Adzhubei IA, Schmidt S, Peshkin L, Ramensky VE, Gerasimova A, Bork P *et al* (2010) A method and server for predicting damaging missense mutations. *Nat Methods* **7**:248–249.
- Badiali M, Gleize V, Paris S, Moi L, Elhouadani S, Arcella A *et al* (2012) KIAA1549-BRAF fusions and IDH mutations can coexist in diffuse gliomas of adults. *Brain Pathol* **22**:841–847.
- Cerami E, Gao J, Dogrusoz U, Gross BE, Sumer SO, Aksoy BA *et al* (2012) The cBio cancer genomics portal: an open platform for exploring multidimensional cancer genomics data. *Cancer Discov* **2**:401–404.
- Ferrer-Costa C, Gelpi JL, Zamakola L, Parraga I, de IC X, Orozco M (2005) PMUT: a web-based tool for the annotation of pathological mutations on proteins. *Bioinformatics* **21**:3176–3178.
- Frazier DP, Kendig RD, Kai F, Maglic D, Sugiyama T, Morgan RL *et al* (2012) Dmp1 physically interacts with p53 and positively regulates p53's stability, nuclear localization, and function. *Cancer Res* **72**:1740–1750.
- Gao J, Aksoy BA, Dogrusoz U, Dresdner G, Gross B, Sumer SO *et al* (2013) Integrative analysis of complex cancer genomics and clinical profiles using the cBioPortal. *Sci Signal* **6**:p11.
- Giacomazzi CR, Giacomazzi J, Netto CB, Santos-Silva P, Selistre SG, Maia AL *et al* (2015) Pediatric cancer and Li–Fraumeni/Li–Fraumeni-like syndromes: a review for the pediatrician. *Rev Assoc Med Bras* **61**:282–289.
- Herman JG, Graff JR, Myohanen S, Nelkin BD, Baylin SB (1996) Methylation-specific PCR: a novel PCR assay for methylation status of CpG islands. *Proc Natl Acad Sci U S A* **93**:9821–9826.
- Jeong SJ, Dasgupta A, Jung KJ, Um JH, Burke A, Park HU, Brady JN (2008) PI3K/AKT inhibition induces caspase-dependent apoptosis in HTLV-1-transformed cells. *Virology* **370**:264–272.
- Jimbo A, Fujita E, Kourouki Y, Ohnishi J, Inohara N, Kuida K *et al* (2003) ER stress induces caspase-8 activation, stimulating cytochrome c release and caspase-9 activation. *Exp Cell Res* **283**:156–166.
- Kent WJ, Sugnet CW, Furey TS, Roskin KM, Pringle TH, Zahler AM, Haussler D (2002) The human genome browser at UCSC. *Genome Res* **12**:996–1006.
- Kim YH, Nobusawa S, Mittelbronn M, Paulus W, Brokinkel B, Keyvani K *et al* (2010) Molecular classification of low-grade diffuse gliomas. *Am J Pathol* **177**:2708–2714.
- Kim YH, Ohta T, Oh JE, Le Calvez-Kelm F, McKay J, Voegelé C *et al* (2014) TP53, MSH4, and LATS1 germline mutations in a family with clustering of nervous system tumors. *Am J Pathol* **184**:2374–2381.
- Kircher M, Witten DM, Jain P, O’Roak BJ, Cooper GM, Shendure J (2014) A general framework for estimating the relative pathogenicity of human genetic variants. *Nat Genet* **46**:310–315.
- Kumar P, Henikoff S, Ng PC (2009) Predicting the effects of coding non-synonymous variants on protein function using the SIFT algorithm. *Nat Protoc* **4**:1073–1081.
- Louis DN, Ohgaki H, Wiestler OD, Cavenee WK (eds) (2007) *WHO Classification of Tumours of the Central Nervous System*, IARC: Lyon
- Malkin D (2011) Li–Fraumeni syndrome. *Genes Cancer* **2**:475–484.
- McCubrey JA, Steelman LS, Abrams SL, Bertrand FE, Ludwig DE, Basecke J *et al* (2008) Targeting survival cascades induced by activation of Ras/Raf/MEK/ERK, PI3K/PTEN/Akt/mTOR and Jak/STAT pathways for effective leukemia therapy. *Leukemia* **22**:708–722.
- McIlwain DR, Berger T, Mak TW (2013) Caspase functions in cell death and disease. *Cold Spring Harb Perspect Biol* **5**:a008656.
- Muller A, Holzmann K, Kestler HA (2007) Visualization of genomic aberrations using Affymetrix SNP arrays. *Bioinformatics* **23**:496–497.
- Nakamura M, Watanabe T, Klangby U, Asker CE, Wiman KG, Yonekawa Y *et al* (2001) *P14Arf* deletion and methylation in genetic pathways to glioblastomas. *Brain Pathol* **11**:159–168.



22. Ng PC, Henikoff S (2003) SIFT: predicting amino acid changes that affect protein function. *Nucleic Acids Res* **31**:3812–3814.
23. Ohgaki H (2009) Epidemiology of brain tumors. *Methods Mol Biol* **472**:323–342.
24. Ohgaki H, Kim YH, Steinbach JP (2010) Nervous system tumors associated with familial tumor syndromes. *Curr Opin Neurol* **23**: 583–591.
25. Ohgaki H, Kleihues P (2005) Population-based studies on incidence, survival rates, and genetic alterations in astrocytic and oligodendroglial gliomas. *J Neuropathol Exp Neurol* **64**:479–489.
26. Ostrom QT, Bauchet L, Davis FG, Deltour I, Fisher JL, Langer CE *et al* (2014) The epidemiology of glioma in adults: a “state of the science” review. *Neuro Oncol* **16**:896–913.
27. Ostrom QT, Gittleman H, Farah P, Ondracek A, Chen Y, Wolinsky Y *et al* (2013) CBTRUS statistical report: primary brain and central nervous system tumors diagnosed in the United States in 2006–2010. *Neuro Oncol* **15**(Suppl2):ii1–ii56.
28. Park JY, Park JM, Jang JS, Choi JE, Kim KM, Cha SI *et al* (2006) Caspase 9 promoter polymorphisms and risk of primary lung cancer. *Hum Mol Genet* **15**:1963–1971.
29. Rotem-Bamberger S, Katz C, Friedler A (2013) Regulation of ASPP2 interaction with p53 core domain by an intramolecular autoinhibitory mechanism. *PLoS One* **8**:e58470.
30. Shiozaki EN, Chai J, Shi Y (2002) Oligomerization and activation of caspase-9, induced by Apaf-1 CARD. *Proc Natl Acad Sci U S A* **99**: 4197–4202.
31. Soengas MS, Alarcon RM, Yoshida H, Giaccia AJ, Hakem R, Mak TW, Lowe SW (1999) Apaf-1 and caspase-9 in p53-dependent apoptosis and tumor inhibition. *Science* **284**:156–159.
32. Stupp R, Mason WP, van den Bent MJ, Weller M, Fisher B, Taphoorn MJ *et al* (2005) Radiotherapy plus concomitant and adjuvant temozolomide for glioblastoma. *N Engl J Med* **352**:987–996.
33. Trigiante G, Lu X (2006) ASPP [corrected] and cancer. *Nat Rev Cancer* **6**:217–226.
34. Vital A, Bringuier PP, Huang H, San Galli F, Rivel J, Ansoberlo S *et al* (1998) Astrocytomas and choroid plexus tumors in two families with identical *p53* germline mutations. *J Neuropathol Exp Neurol* **57**: 1061–1069.
35. Watanabe K, Tachibana O, Sato K, Yonekawa Y, Kleihues P, Ohgaki H (1996) Overexpression of the EGF receptor and p53 mutations are mutually exclusive in the evolution of primary and secondary glioblastomas. *Brain Pathol* **6**:217–224.
36. Watanabe T, Nobusawa S, Kleihues P, Ohgaki H (2009) IDH1 mutations are early events in the development of astrocytomas and oligodendrogliomas. *Am J Pathol* **174**: 1149–1153.
37. Watanabe T, Vital A, Nobusawa S, Kleihues P, Ohgaki H (2009) Selective acquisition of IDH1 R132C mutations in astrocytomas associated with Li–Fraumeni syndrome. *Acta Neuropathol* **117**: 653–656.
38. Xing EP, Nie Y, Song Y, Yang GY, Cai YC, Wang LD, Yang CS (1999) Mechanisms of inactivation of *p14ARF*, *p15 INK4b*, and *p16INK4a* genes in human esophageal squamous cell carcinoma. *Clin Cancer Res* **5**:2704–2713.
39. Yates A, Akanni W, Amode MR, Barrell D, Billis K, Carvalho-Silva D *et al* (2016) Ensembl 2016. *Nucleic Acids Res* **44**:D710–D716.
40. Zawlik I, Vaccarella S, Kita D, Mittelbronn M, Franceschi S, Ohgaki H (2009) Promoter methylation and polymorphisms of the *MGMT* gene in glioblastomas: a population-based study. *Neuroepidemiology* **32**:21–29.

## SUPPORTING INFORMATION

Additional Supporting Information may be found in the online version of this article at the publisher’s web-site:

**Table S1.** Primer sequences for Sanger sequencing.